Original Article

Isolation, characterization and modulatory potentials of β-stigmasterol, ergosterol and xylopic acid from *Anchomanes difformis* on mitochondrial permeability transition pore *in vitro*

Kehinde Oluseun Sodeinde [a,*], Akinwunmi Oluwaseun Adeoye [b,*], Adedeji Adesipo [a], Adebayo A. Adeniyi [a,d], John Adeolu Falode [b], Tajudeen Olabisi Obafemi [c], Samuel Olalekan Olusanya [a], Linette Twigge [d], Jeanet Conradie [d], Timothy O. Mosaku [e]

[a] Department of Chemistry, Federal University Oye-Ekiti, Ekiti State 371104, Nigeria
[b] Biomembrane, Toxicology and Drug Discovery Unit, Department of Biochemistry, Federal University Oye-Ekiti, Ekiti State 371104, Nigeria
[c] Department of Biochemistry, Afe Babalola University, Ado-Ekiti, Ekiti State 360001, Nigeria
[d] Department of Chemistry, University of Free State, Bloemfontein 9301, South Africa
[e] Department of Civil Engineering, Covenant University, Ogun State 112104, Nigeria

ARTICLE INFO

ABSTRACT

Objective: Secondary metabolites and polyphenolic compounds from medicinal plants have been demonstrated to have multiple biological functions with promising research and development prospects. This study examined the effect of β-stigmasterol (with ergosterol) and xylopic acid isolated from *Anchomanes difformis* on liver mitochondrial permeability transition pore (mPTP).
Methods: The compounds were isolated by vacuum liquid chromatography. Mitochondrial swelling was assessed as changes in absorbance under succinate-energized conditions.
Results: ^{1}H and ^{13}C NMR spectroscopic elucidation of the isolates affirmed the presence of β-stigmasterol with ergosterol (1:0.3) and xylopic acid. The isolates reversed the increase in lipid peroxidation and inhibited the opening of mitochondrial permeability transition pores caused by calcium and glucose. Pharmacological inhibition of mPTP offers a promising therapeutic target for the treatment of mitochondrial-associated disorders.
Conclusion: Reduction in the activity of calcium ATPase and the expression of Caspase-3 and −9 were observed, suggesting that they could play a role in protecting physicochemical properties of membrane bilayers from free radical-induced severe cellular damage and be useful in the management of diseases where much apoptosis occurs.

1. Introduction

Mitochondria perform several functions as diverse as energy production, fatty acid β-oxidation, reactive oxygen species (ROS) production and detoxification, as well as cell death regulation. The coordination of these functions relies on independent mitochondrial processes as well as continued cross-talk with other organelles and/or cytosol. Consequently, tight regulation of mitochondrial functions ensures cell homeostasis (Zorov, Juhaszova, & Sollott, 2014).

Mitochondrial membrane permeability transition (MPT) pore opening disrupts the proton gradient of the intermembrane space designed by the electron transport chain of the inner mitochondria membrane, therefore resulting in uncoupling oxidative phosphorylation, rupture of the outer mitochondrial membrane, the release of apoptogenic proteins such as cytochrome *C*, apoptosis-inducing factor, and small mitochondrial-dependent activator of caspase (Zorov et al., 2014; Halestrap, McStay & Clarke, 2002).

An increase in intracellular calcium concentration and higher concentrations of inorganic phosphate had been implicated in the opening of the mitochondrial permeability transition pore (mPTP). A high concentration of glucose leads to hyperglycemia and over time, could reduce the insulin secretion capacity of pancreatic β-cells, and the subsequent increase in insulin resistance leads to further hyperglycemia which will eventually result in oxidative stress (Dubois, Vacher, Roger, Huyghe, & Vandewalle, 2007). Evidence demonstrates that some toxicants increase their

* Corresponding authors.
E-mail addresses: kehinde.sodeinde@fuoye.edu.ng (K.O. Sodeinde), akinwunmi.adeoye@fuoye.edu.ng (A.O. Adeoye).

carcinogenicity via oxidative stress. A high concentration of toxicants can induce mitochondrial swelling, decrease the membrane potential, enhance the permeability of H^+ and K^+, and induce membrane lipid peroxidation (Fan et al., 2018).

Higher intracellular calcium concentration coupled with oxidative stress lead to the opening of permeability transition pore and ultimately leads to cell death through pathophysiological conditions such as drug toxicity and neurodegenerative diseases (Bernardi, Rasola, Forte, & Lippe, 2015). Inhibition and induction of the MPT pore are well implicated with diseases associated with uncontrolled cell growth (including Alzheimer, motor neuron, spinal muscular atrophy, etc) and cell death (Srinivasan, 2012). Bioactive compounds from medicinal plants have been reported to serve as modulators of the MPT pore and are valuable in the pharmacological targeting of mitochondria (Adeoye, Falode, Jeje, Agbetuyi-Tayo, & Giwa, 2022; Devendra & Leng, 2011; Fulda, 2010).

Anchomanes difformis (Blume) Engl. belongs to the family Araceae and is a native of West African countries including Nigeria, Ghana, and Senegal (Adebayo, John-Africa, Agbafor, Omotosho, & Mosaku, 2014). It is commonly known as igolangbodo, ogiriosako (in South Western Nigeria), forest anchomanes, etc (Adebayo, John-Africa, Agbafor, Omotosho, & Mosaku, 2014). It is a large herbaceous perennial plant with a stout prickly stem of about 0.8 to 2 m high (Akinkurolere, Adedire & Odeyemi, 2006). The plant has been reported to possess antimalarial, anti-inflammatory, antimicrobial, and antinociceptive properties (Oyetayo, 2007). Phytochemical screening of *A. difformis* extracts confirmed the presence of alkaloids, terpenoids, tannins, saponins, and flavonoids (Oyetayo, 2007). Stigmasterol is a plant lipid whose chemical structure is similar to that of cholesterol but with slight modifications. Several studies have reported its use as a therapeutic mediator in the treatment of various diseases as an antipyretic, anti-cancer, anti-atherosclerotic cholesterol-lowering, anti-inflammatory, and immune-modulating agents (Sabeva, McPhaul, Li, Cory, & Feola, 2011; Bouic, Etsebeth, Liebenberg, Albrecht, & Pegel, 1996). Xylopic acid is a kaurene diterpene with analgesic, antimalarial and antipyretic properties (Boampong, Ameyaw, Aboagye, Asare, & Kyei, 2013). There have been continuous research efforts toward the identification of potent bioactive agents from medicinal and dietary plants that can modulate the mitochondria MPT pore. Despite the properties exhibited by both stigmasterol and xylopic acid, it is not yet known whether they could modulate the opening of the transition pore and thus alleviate excessive tissue wastage in neurodegenerative disease conditions. This study, therefore, investigated the isolation and characterization of β-stigmasterol (with ergosterol) and xylopic acid from *A. difformis* and their effects on MPT pore *in vitro*.

2. Materials and methods

2.1. Chemicals and reagents

Methanol, *n*-hexane, chloroform, ethyl acetate, silica gel, mannitol sucrose, ethyl glycol tetraacetic acid (EGTA), 4-2-hydroxyethyl piperazine-1-ethane sulfonic acid (HEPES), spermine, rotenone, and succinate were purchased from Sigma-Aldrich Company (St. Louis, MO, USA). BSA (bovine serum albumin), calcium chloride, sodium hydroxide, sodium carbonate, copper sulfate, phosphate buffer, Folin C and other reagents used were of analytical grade.

2.2. Plant material collection

A. difformis plant sample was collected at Odo Oro, Ikole-Ekiti, Ekiti State, Nigeria. The sample was air-dried in the laboratory at

room temperature and relative humidity of about 50%. The dried leaves and stems were pulverized separately and stored in clean glass vials.

2.3. Extraction of crude extract from plant sample

Pulverized leaves (about 950 g) and stems (570 g) of *A. difformis* were each transferred into separate glass containers, respectively. A total of 5 L of methanol was added to each container, stirred for 2 h, and allowed to stand for 72 h. The resulting solution mixtures were filtered using a porcelain filter with a fine-pored muslin cloth. The filtrate in each case was concentrated in a vacuum oven at 40 °C. The percentage yield was 42 g (4.4%) for the leaf and 16 g (2.8%) for the stem. The concentrated crude methanolic extract was treated with 200 mL of 50% of the methanolic solution in a separating funnel. The *n*-hexane solution (200 mL) was subsequently added to the funnel and carefully shaken for equilibration. The resulting mixture was allowed to stand for 10 min to ensure proper partitioning of the two phases. The hexane layer (at the top) was collected after releasing the methanol/water layer (bottom). This process was repeated until a clear layer was obtained for the hexane portion. Isolated fractions were concentrated using a rotary evaporator and vacuum oven respectively at 40 °C. The yield obtained from the *n*-hexane stem fraction (L1) was 5.8 g and 10.2 g for the methanol residue (L2). The yield obtained from the *n*-hexane leaf fraction (L3) was 25.4 g and 16.6 g for the methanol residue of the leaf (L4). Only samples L1 and L4 were subjected to further studies.

2.4. Isolation of pure compounds from hexane and methanol fractions

The 5 g of the *n*-hexane stem fraction (L1) was subjected to further purification by vacuum liquid chromatography (VLC). The hexane fraction was pre-absorbed with 100 mL of *n*-hexane and added 100 g of silica gel GF$_{254}$. The mixture was allowed to dry and packed in a sintered glass which has been packed with 200 g of silica gel with the aid of a vacuum pump. Elution of the components was achieved using 500 mL of each of the following solvent systems of increasing polarity: *n*-hexane, *n*-hexane/chloroform, chloroform/ethylacetate, ethylacetate/methanol until the extract was fully eluted. The obtained fractions were concentrated using a rotary evaporator at 40 °C. Crystals from fraction 2 were collected, washed with methanol, and dried under a vacuum. The same procedure was repeated for methanol leaf fraction (L4).

2.5. NMR characterization of compounds

The ^{1}H and ^{13}C NMR spectra of the isolated compounds (from samples L1 and L4) were recorded at 25.0 °C on a 600 MHz Avance II Bruker NMR spectrometer (Console/DRX 600, Mundelein, Illinois USA) operating at 600.28 MHz for ^{1}H and 150.95 MHz for ^{13}C using deuterated chloroform. The chemical shifts (δ) are reported in parts per million ($\times 10^{-6}$) and the spectra were referenced relative to the tetramethylsilane (TMS), Me_4Si internal standard at 0 ppm.

2.6. Experimental animals

Eighteen normal male albino rats (Wistar strain) weighing between 100 and 150 g were obtained from Animal Colony, Department of Science Technology, Federal Polytechnic Ado-Ekiti, Ekiti State, Nigeria. Animals were maintained in controlled well-ventilated plastic cages and were given grower mash and water *ad libitum*. They were allowed to acclimatize for one week at the Animal House, Department of Biochemistry, Federal University Oye-Ekiti, Ekiti State, Nigeria before the *in vitro* experiments. Ethical approval and the license for the use of animals were approved by the Faculty of Science, Federal University Oye-Ekiti ethical

review committee (Approval Number: FAS/BCH2021026). All procedures in this study conformed to the guiding principles for research involving animals as recommended by the Declaration of Helsinki and the National Institute of Health.

2.7. Biochemical analysis

Low-ionic-strength liver mitochondria were isolated as previously described by Johnson and Lardy (1967). The mitochondrial protein was estimated as previously described according to Lowry, Rosebrough, Farr & Randall (1951) using Bovine Serum Albumin (BSA) as standard. Mitochondrial swelling was assessed according to the method described by Lapidus and Sokolove (1993). Lipid peroxidation assay was done using the method of Ruberto, Baratta, Deans & Dorma (2000). Cytochrome *C* release from isolated mitochondria was carried out and estimated from a standard curve according to Appaix, Minatchy, Riva-Laveille, Olivares & Antosson (2000). Caspase-3 and Caspase-9 were done using rat-specific ELISA kits according to McKenzie, Fernandes, Doan, Schmitt & Brandon (2021). Calcium ATPase activity was measured using the method of Lin and Way (1982).

2.8. Statistical analysis

Data were analyzed by one-way ANOVA with Dunnett's multiple comparison post hoc test to compare groups with one independent variable. Data were analyzed using Graphpad Prism 5.0 version. All data were presented as mean ± standard error of the mean (SEM). The level of significance was set at $P < 0.05$.

3. Results

3.1. Identification of compounds by 1D NMR (^1H, ^{13}C) and 2D NMR spectroscopy

Two white solid samples were isolated from the *n*-hexane fraction of stems (L1) and the methanol fraction of leaves (L4) of *A. difformis* respectively. Both 1D NMR (^1H, ^{13}C) and 2D NMR (COSY, HMBC, HSQC) of the isolates were carried out for structural elucidation. The isolates from L1 were identified to be a mixture of *β*-stigmasterol (**L1a**; molecular weight = 412.69 g/mol) and ergosterol (**L1b**; molecular weight = 396.65 g/mol) (Fig. 1) in the ratio of 1:0.3 according to the integration of their ^1H NMR resonance, especially for the observed resonance of H-3 (1H, 3.53, m) and H-4 (2H, 2.30, ddd, *J* = 13.2, 5.2, 2.1 Hz) for **L1a** and found at 3.64 (m) and 2.47 (ddd, *J* = 14.3, 4.7, 2.5 Hz) respectively for **L1b** as shown in Fig. S1. The details of all the ^1H and ^{13}C NMR were shown in Table 1 for the two identified compounds in sample L1. The ^{13}C NMR also clearly showed the difference in the resonance of the **L1a** and **L1b** mixture as indicated in Fig. S2. Some of the distinguishing features of the two compounds in the mixture were C-5 (140.77,

*139.80), C-6 (121.73, *119.60), C-7(31.9, *116.30), C-22 (138.32, *135.58), C-23 (129.29, *131.99). The values with superscript '*' are for the L1b compound. The results of the 2D NMR COSY, HSQC, and HMBC for sample 1 were added to the supplementary data as Figs. S3–S5 respectively for the mixture of **L1a** and **L1b**. One of the most distinguishing features of the **L1b** from **L1a** is the correlation of its $^1H/^{13}C$ for CH at C-7 as indicated in HSQC which is found in the upper field compared with that of **L1a** which is found in the lower field (Fig. S5). Another was the $^1H/^1H$ NMR from COSY showing the correlation of H-6 and H-7 in **L1b** (Fig. S3). The second isolate from sample L4 was identified to be a pure compound of xylopic acid (**XL4**, molecular weight = 360.5 g/mol, refractive index = 1.55). The ^1H and ^{13}C NMR were shown in Figs. S6 and S7, respectively.

The 2D NMR COSY, HMBC, and HSQC were added to the supplementary data as Figs. S8–S10. The details of all the ^1H and ^{13}C NMR that characterized the **XL4** molecules were shown in Table 1. Among the important resonance were those of H-1 (2H, 0.89, td, *J* = 13.0, 3.7 Hz), H-3 (2H, 1.03, td, *J* = 13.7, 4.4 Hz), H-7 (2H, 1.18, dd, *J* = 11.8, 4.5), H-9 (1H, 1.33 (d, *J* = 7.1 Hz), H-14 (2H, 1.39, td, *J* = 13.4, 3.9, 1.47 Hz), H-18 (3H, 1.24, s) and H-20 (3H, 0.98, s) that were shown in Fig. S8 and those of carbon C-5 (56.50), C-9 (46.98), C-11 (18.01), C-15 (81.66), C-16 (153.76), C-17 (106.12), C-18 (28.90), C-19 (184.42), C-20 (15.85), C-21 (171.44), C-22 (21.32). Among the identified $^1H/^{13}C$ correlation in the 2D HMBC are the correlation of H-22/C-21 and H-18/C-19 and H-6/C-19 as indicated in Fig S9. In the HSQC NMR, the C-17/H-17 (CH$_2$) and C-15/H-15 (CH), C-13/H-13 (CH), C-5/H-5 (CH), and C-20/H-20 (CH3) as shown in Fig. S10 differentiating CH$_2$ (blue) from CH (red).

3.2. Assessment of mitochondrial intactness

Fig. 2 depicted the assessment of calcium (the reference triggering agent) and high glucose concentration as well as spermine (the reference inhibitor) on permeability transition pores in normal rat liver mitochondria. No significant change was observed in the absorbance of mitochondrial within 12 min recorded at 540 nm in the absence of calcium. This implies the intactness (integrity) of the mitochondria, i.e., there was no induction of membrane permeability transition pore opening of mitochondrial energized with succinate. The result showed a drastic reduction in absorbance at 540 nm in the presence of exogenous calcium and glucose, indicating a large amplitude mitochondrial swelling with an induction fold of 22.61 and 8.39 respectively, which was significantly inhibited by spermine with 87.48% inhibition.

3.2.1. Effect of β-stigmasterol (with ergosterol) on permeability transition pores in presence and absence of calcium

The effect of varying concentrations (10, 20, 32, and 45 µg/mL) of *β*-stigmasterol (with ergosterol) i.e. **L1** (**a** & **b**) on the permeabil-

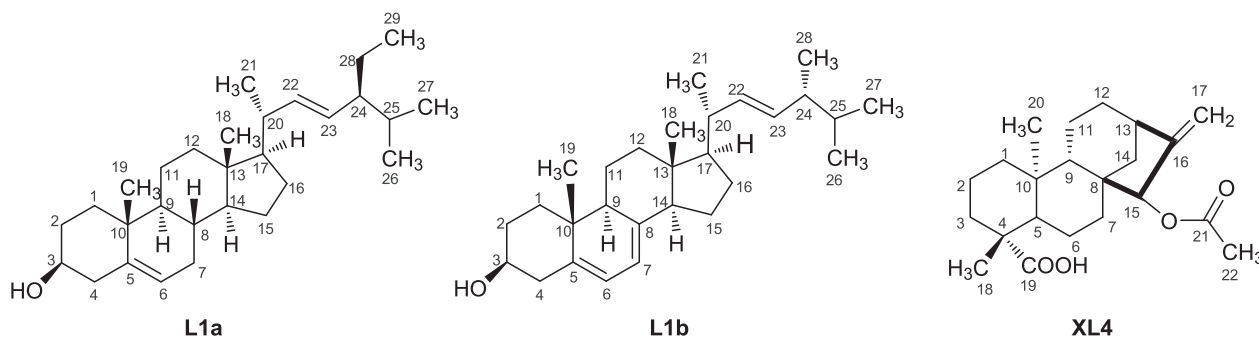**Fig. 1.** Structures of *β*-stigmasterol (**L1a**), ergosterol (**L1b**), and xylopic acid (**XL4**) isolated from *A. difformis*.

Table 1
^{1}H and ^{13}C NMR data for compounds L1a, L1b, and XL4 (in CDCl$_3$, 600.28 and 150.95 MHz for ^{1}H and ^{13}C).

No.	L1a		L1b		XL4	
	δ_H	δ_C	δ_H	δ_C	δ_H	δ_C
1		37.3		38.4	0.89 (td, J = 13.0, 3.7 Hz)1.94 (d, J = 14.1 Hz)	40.8
2		31.7		32.0	1.46 1.90	19.1
3	3.53 (m)	71.8	3.64 (m)	70.5	1.03 (td, J = 13.7, 4.4 Hz) 1.24	37.7
4	2.30 (ddd, J = 13.2, 5.2, 2.1 Hz)2.23 (m)	42.2	2.47 (ddd, J = 14.3, 4.7, 2.5 Hz)2.28 (m)	40.8	–	43.7
5		140.8		139.8	1.02 (d, J = 11.8 Hz)	56.5
6	5.35 (m)	121.7	5.38 (m)	119.6	1.80 1.88	21.3
7		31.9	5.57 (dd, J = 5.6, 2.3 Hz)	116.3	2.07 (d, J = 11.8 Hz)1.18 (dd, J = 11.8, 4.5 Hz)	36.4
8		31.9		141.4	–	46.0
9		51.3		46.3	1.33 (d, J = 7.1 Hz)	47.0
10		36.5		37.0	–	39.4
11		21.2		21.1	1.57 1.69	18.0
12		39.9		39.1	1.49 1.65	33.3
13		42.3		42.8	2.67 (br s)	40.6
14		56.9		54.6	1.39 (td, J = 13.4, 3.9 Hz) 1.47)	38.9
15		24.4		23.0	5.15 (t, J = 1.5 Hz)	81.7
16		28.9		28.3	–	153.8
17		56.1		55.8	4.94 (d, J = 2.5 Hz)4.87 (br s)	106.1
18		12.3		12.0	1.24 (s)	28.9
19		19.8		17.6	–	184.4
20		40.5		40.4	0.98 (s)	15.8
21		21.1		21.1	–	171.4
22	5.15 (dd, J = 15.3, 8.4 Hz)	138.3	5.23 (dd, J = 15.2, 7.3 Hz)	135.6	2.17 (s)	21.3
23	5.02 (dd, J = 15.3, 8.5 Hz)	129.3	5.18 (dd, J = 15.2, 7.3 Hz)	132.0	–	–
24		50.2		42.8	–	–
25		34.0		33.1	–	–
26		23.1		19.7	–	–
27		19.4		20.0	–	–
28		26.1		16.3	–	–
29		12.1		–	–	–

Note: Chemical shifts are given in (ppm) relative to an internal reference, tetramethylsilane (TMS). Coupling constants (J) are given in Hz.
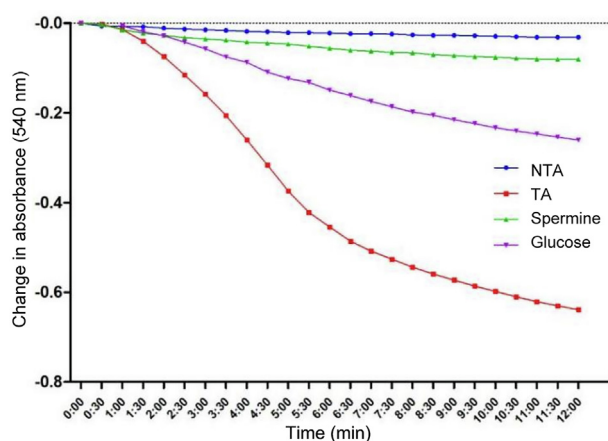

Fig. 2. Induction of mitochondrial membrane permeability transition pore opening by calcium and glucose and reversal by spermine in normal rat liver mitochondria. NTA: Non-triggering agent; TA: Triggering agent (Calcium).

ity transition pores in the absence, and presence of exogenous calcium and glucose were presented in Fig. 3. In the absence of calcium, **L1** (**a** & **b**) significantly inhibited the mitochondrial permeability transition pores at all concentrations tested (Fig. 3A). The percentage inhibition for **L1** (**a** & **b**) in the absence of calcium at (10, 20, 32, and 45 μg/mL) are 94.05%, 94.68%, 90.77%, and 83.72% respectively. In the presence of calcium and glucose, **L1** (**a** & **b**) exhibited a mild inductive effect in a concentration-dependent manner. However, this mild inductive effect was higher in the presence of calcium when compared with the presence of glucose (Fig. 3B and C).

3.2.2. Effect of xylopic acid on permeability transition pores in presence and absence of calcium

The effect of varying concentrations (10, 20, 32, and 45 μg/mL) of xylopic acid (**XL4**) on the permeability transition pores in the absence and presence of exogenous calcium and glucose was shown in Fig. 4. In the absence of calcium, xylopic acid significantly inhibited the MPT pores at all concentrations tested. The percentage inhibition for sample **L1** (**a** & **b**) in the absence of calcium at (10, 20, 32, and 45 μg/mL) were 96.09%, 96.40%, 94.52%, and 86.07% respectively (Fig. 4A). In the presence of calcium and glucose, xylopic acid also revealed a mild inductive effect in a concentration-dependent manner. In this way with sample **L1** (**a** & **b**), the mild inductive effect observed for **XL4** was also higher in the presence of calcium when compared with the presence of glucose (Fig. 4B and C).

3.2.3. Effects of β-stigmasterol (with ergosterol) and xylopic acid on cytochrome C release

From the results, the release of cytochrome *c* from calcium (the reference standard) and glucose was significant when com-
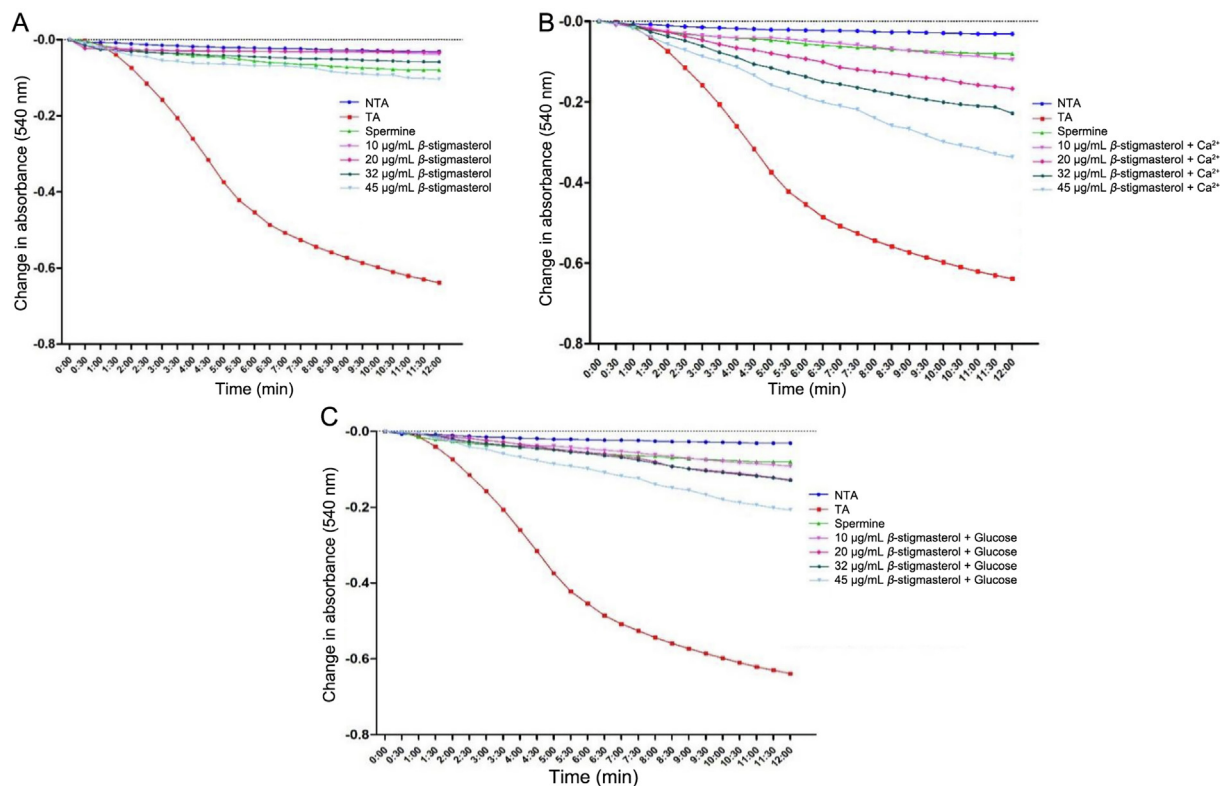
Fig. 3. Effect of various concentrations of β-stigmasterol (with ergosterol) (sample **L1 a** & **b**) on mitochondrial membrane permeability transition pore in the absence and presence of calcium and glucose. NTA: Non-triggering agent; TA: Triggering agent, +Ca^{2+}: in the presence of calcium.
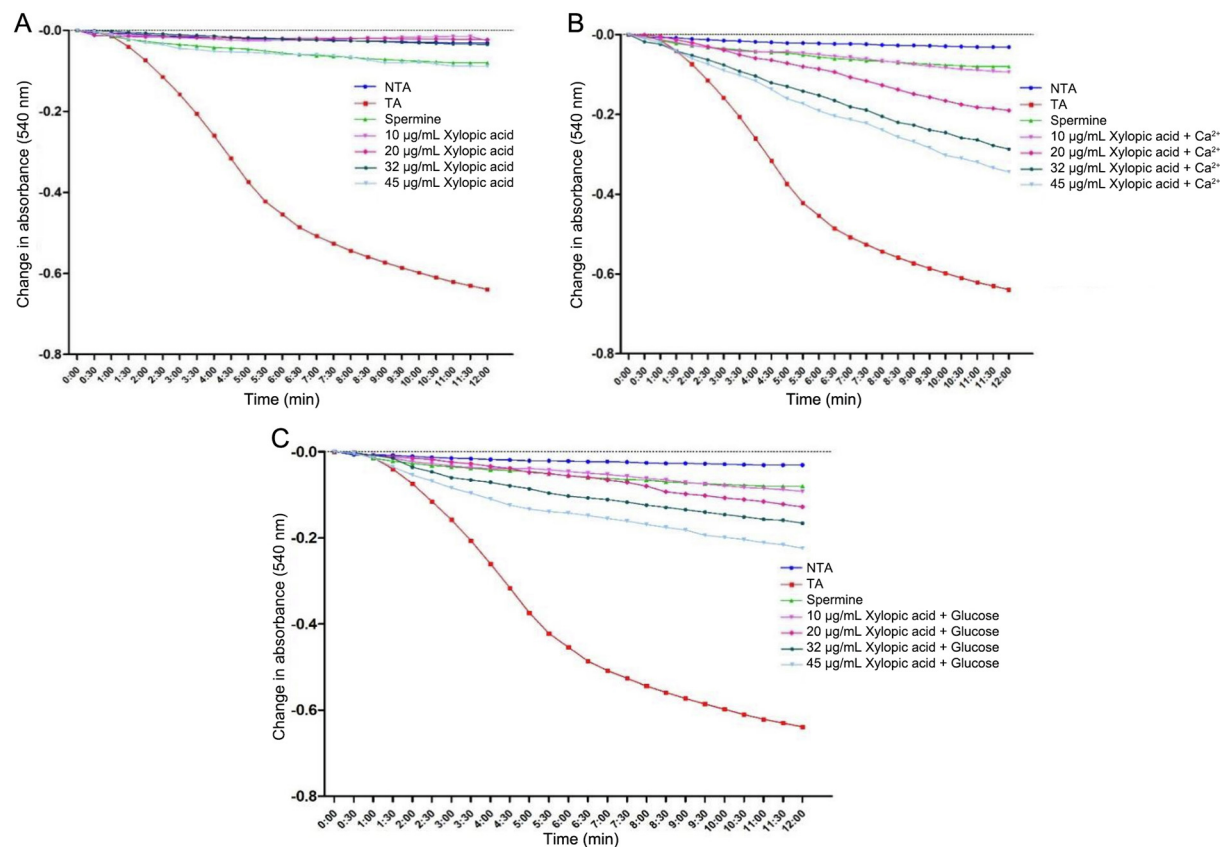

Fig. 4. Effect of various concentrations of xylopic acid (**XL4**) on mitochondrial MPT pore in the absence and presence of calcium and glucose. NTA: Non-triggering agent; TA: Triggering agent; +Ca^{2+}: in the presence of calcium.

pared with β-stigmasterol (with ergosterol) (sample **L1 a** & **b**) and xylopic acid (sample **XL4**), both in the absence and presence of calcium and glucose respectively (*P* < 0.05). There was no significant induction of cytochrome *C* relwease at the two concentrations (32 and 45 μg/mL) tested for both samples **L1** (**a** & **b**) and **XL4** both in the presence of exogenous calcium and glucose (Fig. 5).

3.3. Mitochondrial lipid peroxidation

The results showed that there was a significant increase in mitochondrial lipid peroxidation in the presence of triggering agents, exogenous calcium, and glucose when compared with the isolated β-stigmasterol (with ergosterol) and xylopic acid at the two concentrations in the absence of the triggering agents

(*P* < 0.05). The concentrations of malondialdehyde in β-stigmasterol (with ergosterol) and xylopic acid were significantly lowered at the two concentrations in the presence of exogenous calcium and glucose when compared with the triggering agents alone (Fig. 6).

3.4. Caspase-3 and -9 activities

A significant *P* < 0.05 increase in the expression of caspase-3 and −9 activities were observed in the presence of triggering agents, exogenous calcium, and glucose when compared with β-stigmasterol (with ergosterol, **L1 a** & **b**) and xylopic acid (**XL4**) at the two concentrations in the absence of the triggering agents. The expression of caspase-3 and −9 activities in β-stigmasterol (with ergosterol, **L1 a** & **b**) and xylopic acid (**XL4**) without the addi-
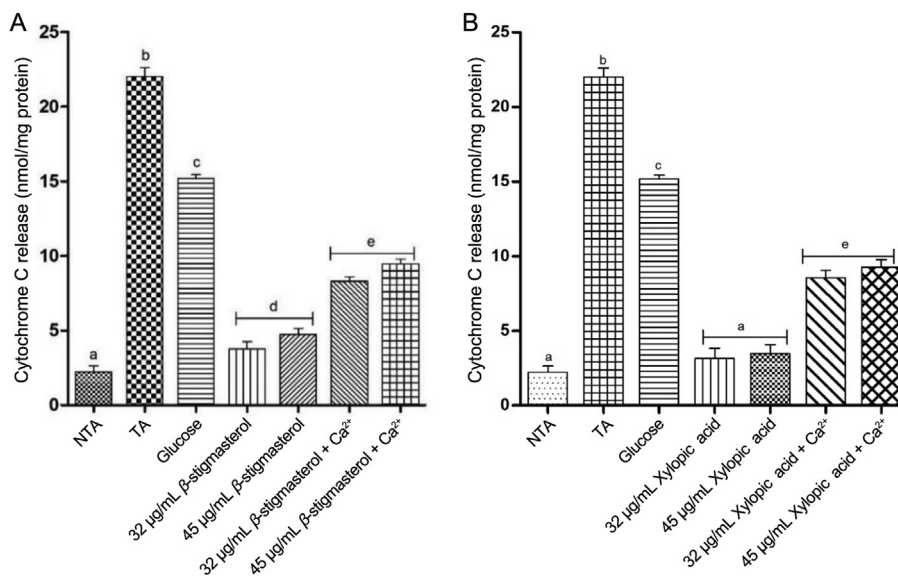

Fig. 5. Effect of various concentrations of β-stigmasterol (with ergosterol) (sample **L1 a** &**b**) and xylopic acid (**XL4**) on normal rat liver mitochondrial cytochrome *c* release (mean ± SEM, *n* = 5). Values with different alphabets are statistically different at *P* < 0.05. NTA: Non-triggering agent; TA: Triggering agent (Calcium).
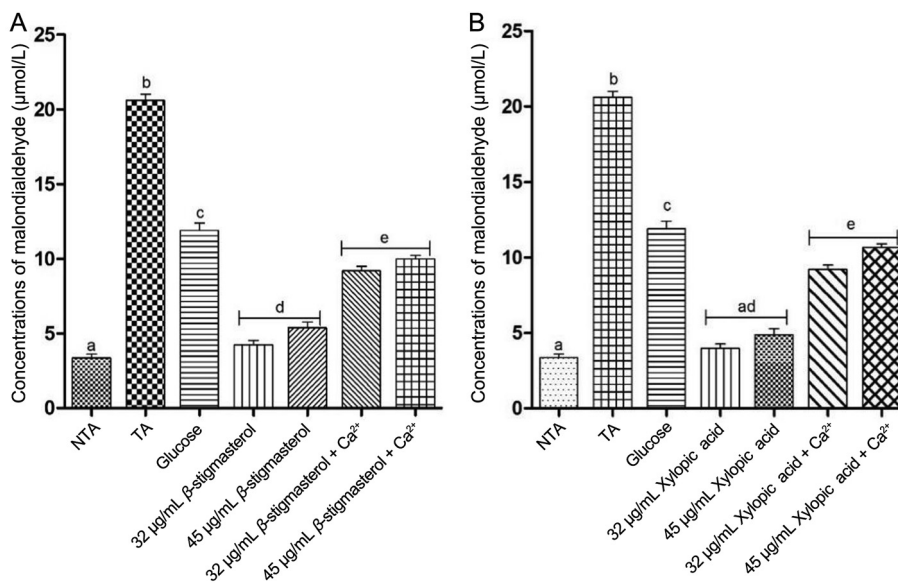

Fig. 6. Effect of various concentrations of β-stigmasterol (with ergosterol) (sample **L1 a** & **b**) and xylopic acid (**XL4**) on normal rat liver mitochondrial lipid peroxidation (mean ± SEM, *n* = 5). Values with different alphabets are statistically different at *P* < 0.05. NTA: Non-triggering agent; TA: Triggering agent (Calcium).

tion of calcium and glucose were found to be lowered at the two concentrations when compared with the triggering agents alone (Fig. 7).

3.5. Calcium ATPase activities

In the same manner, a significant $P < 0.05$ increase in the activities of calcium ATPase was observed in the presence of triggering agents, exogenous calcium, and glucose when compared with stigmasterol and xylopic acid at the two concentrations in the absence of the triggering agents. Calcium ATPase activities in β-stigmasterol and xylopic acid without the addition of calcium and glucose were found to be lowered at the two concentrations when compared with the triggering agents alone (Fig. 8).

4. Discussion

Under normal conditions, the mitochondrial matrix contains CypD and the mPTP remains closed. Its opening is regulated by a plethora of factors, including changes in ionic Ca^{2+}, pH, reactive oxygen species (ROS), adenosine diphosphate/adenosine triphos-

phate (ADP/ATP) levels, and the expression of B-cell lymphoma-2 (Bcl-2), an anti-apoptotic protein (Rao, Carlson, & Yan, 2014). The additive proapoptotic effects of loss of mitochondrial membrane potential and calcium overload in the mitochondria will induce mitochondria permeability transition (MPT) pore opening inevitably. The disturbance of mitochondrial membrane permeability can result in swelling owing to the penetration of the solutes in the matrix (Li, Liu, Zhang, Tian, & Zhao, 2012). From the results of this study (Fig. 2), there was no change in the absorbance of mitochondrial under a succinate-energized condition in the absence of a triggering agent (calcium), which signifies the intactness and integrity of the isolated liver mitochondrial. The observation from this study is in agreement with previous reports (Adeoye, Olanlokun, & Bewaji, 2018; Daniel, Adeoye, Ojowu, & Olorunsogo, 2018). However, in the presence of triggering agents, there was a large-amplitude swelling which was reversed by spermine, a standard inhibitor. Reversal of calcium-induced pore opening by spermine showed that the isolated mitochondria were intact, uncoupled, and therefore suitable for further use. It was observed from the study that exogenous calcium significantly opened the pore when compared with glucose.
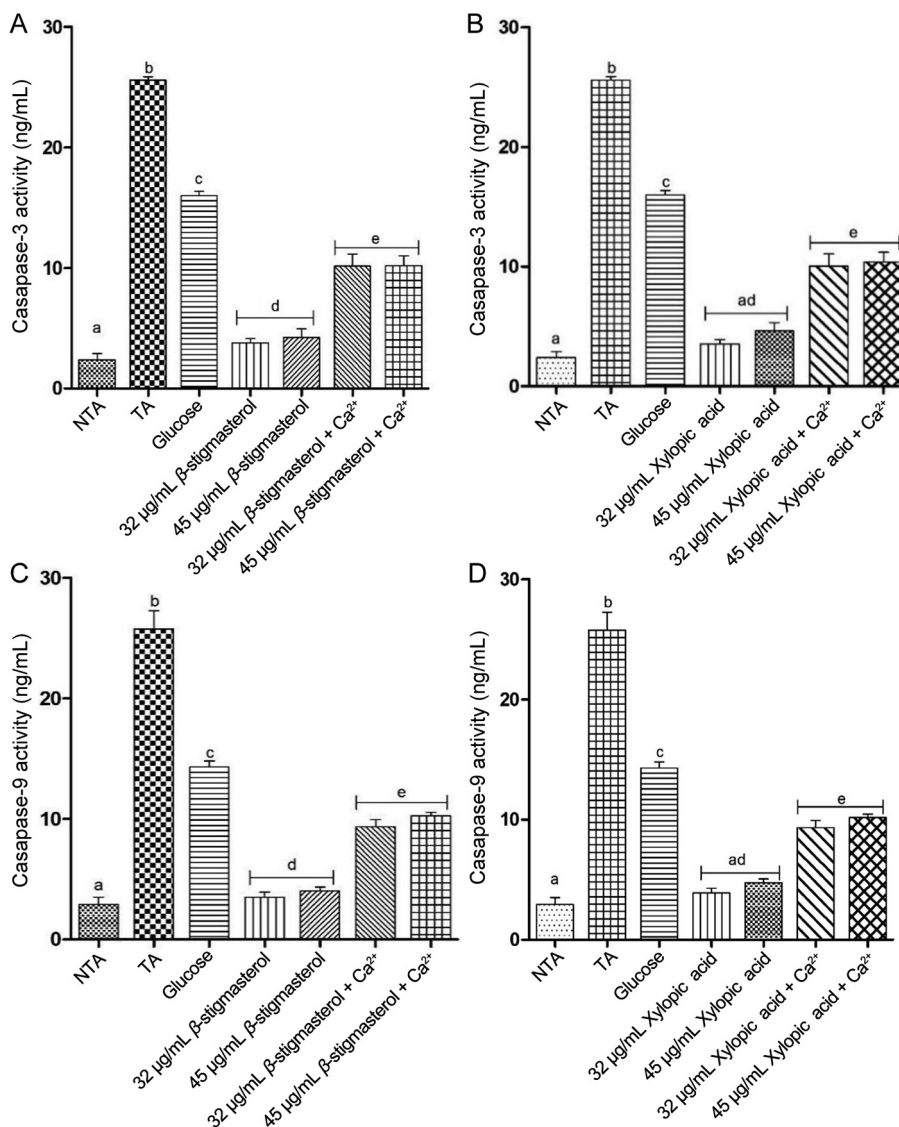

Fig. 7. Effect of various concentrations of β-stigmasterol (with ergosterol) (**L1 a** & **b**) and xylopic acid (**XL4**) on normal rat liver caspase-3 (A, B) and −9 (C, D) activities (mean ± SEM, n = 5). Values with different alphabets are statistically different at $P < 0.05$. NTA: Non-triggering agent; TA: Triggering agent (Calcium).

Fig. 8. Effect of various concentrations of β-stigmasterol (with ergosterol) (**L1 a** & **b**) and xylopic acid (**XL4**) on normal rat liver calcium ATPase activity (mean ± SEM, $n = 5$). Values with different alphabets are statistically different at $P < 0.05$. NTA: Non-triggering agent; TA: Triggering agent (Calcium).
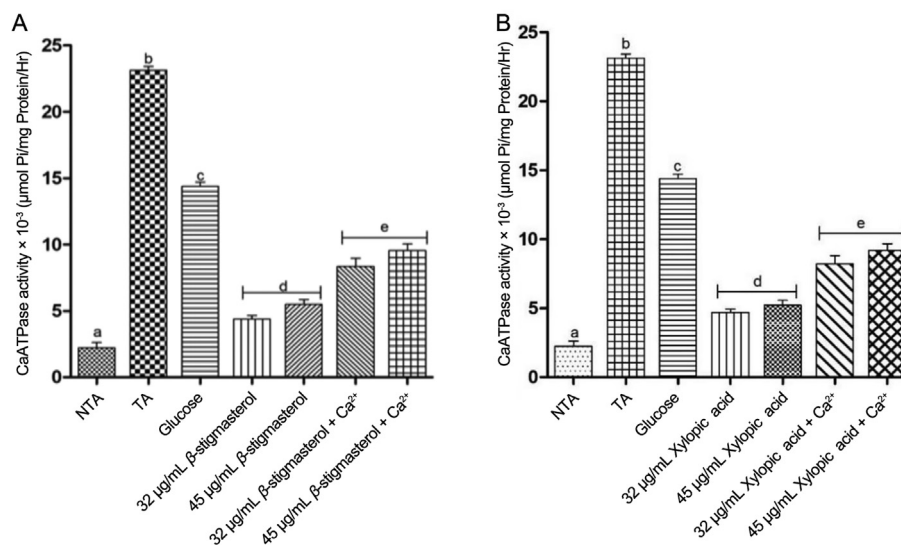
Pharmacological inhibition of mPTP offers a promising therapeutic target for the treatment of mitochondrial-associated disorders (Baines, Kaiser, Purcell, Blair & Osinska, 2005; Morita, Sovari, Xie, Fishbein & Mandel, 2009). Stigmasterol (with ergosterol) and xylopic acid exhibited modulatory effects on the pore opening in the absence of a reference triggering agent; calcium. However, in the presence of calcium and glucose, they contributed to mild induction of the pore opening in a concentration-dependent manner.

The release of cytochrome *C* from mitochondria during apoptosis occurs through the opening of the mitochondria membrane permeability transition pore which is followed by the swelling-induced rupture of the mitochondria outer membrane (Appaix et al., 2000). From the results obtained in this study, there was an increase in cytochrome release in the presence of triggering agents (calcium and glucose) which indicated that there was a significant increase in MPT pore opening. The release of cytochrome *C* in β-stigmasterol (with ergosterol) and xylopic acid, both in the absence and presence of calcium was found to be significantly lower when compared with the triggering agents alone.

Lipid peroxides usually decompose to form aldehydes (e.g. malondialdehyde) which can cross-link or change the structures of proteins, lipids, carbohydrates, and DNA (Alessio, 2000). A significant increase in mitochondrial lipid peroxidation was observed in the presence of triggering agents which is in agreement with the significant opening of the MPT pore. Lipid peroxidation may increase the destructive effect of the MPT in cells since it also promotes mitochondrial swelling and cytochrome *C* release (Ruberto, Baratta, Deans & Dorma, 2000). Stigmasterol (with ergosterol) and xylopic acid inhibited mitochondrial lipid peroxidation at the two concentrations tested both in the absence and presence of calcium when compared with the triggering agents alone. It could be suggested that the isolated β-stigmasterol (with ergosterol) and xylopic acid could play a role in protecting the physicochemical properties of membrane bilayers from free radical-induced severe cellular damage.

Caspases are responsible for the regulation of the death sentence in cells (Yuan, Najafov, & Py, 2016). In the cytosol, cytochrome *C* engages the apoptotic protease activating factor-1 (APAF1) and forms the apoptosome, which activates caspase-9. Caspase-3 is a protein that interacts with caspase-8 and caspase-9. It is encoded by the *CASP3* gene. Caspase-9 is a member of the caspase family of cysteine proteases that have been implicated in

apoptosis and cytokine processing. The results of this study showed that there was a significant increase in the expression of caspase-3 and -9 in the presence of triggering agents. The expression of caspase-3 and -9 activities in β-stigmasterol (with ergosterol) and xylopic acid without the addition of calcium and glucose were found to be lowered at the two concentrations when compared with the triggering agents alone.

Calcium ATPase is a transport protein in the plasma membrane of cells that serves to remove calcium from the cell. It is vital for regulating the amount of calcium within cells (Strehler and Zacharias, 2001). It was observed from the results that calcium ATPase activities increased significantly in the presence of triggering agents compared with β-stigmasterol (with ergosterol) and xylopic acid at the two concentrations in the absence of the triggering agents.

5. Conclusion

The modulatory potentials of β-stigmasterol (with ergosterol) and xylopic acid isolated from *A. difformis* on mitochondrial permeability transition pore *in vitro* were successfully investigated. Detailed ^{1}H and ^{13}C NMR spectra of the isolates confirmed the presence of β-stigmasterol (with ergosterol) and xylopic acid. Both β-stigmasterol (with ergosterol) and xylopic acid reversed the increase in mitochondrial lipid peroxidation and also inhibited the opening of the mitochondrial permeability transition pore caused by calcium and glucose. Furthermore, both isolates caused a reduction in the activity of calcium ATPase as well as the expression of caspase-3 and -9. Hence, β-stigmasterol (with ergosterol) and xylopic acid could play a role in protecting the physicochemical properties of membrane bilayers from free radical-induced severe cellular damage and could also be useful in the management of diseases where too much apoptosis takes place.

CRediT authorship contribution statement

Kehinde Oluseun Sodeinde: Conceptualization, Investigation, Software, Data curation, Writing – review & editing. **Akinwunmi Oluwaseun Adeoye:** Conceptualization, Investigation, Software, Data curation, Writing – review & editing. **Adedeji Adesipo:** Conceptualization, Investigation, Software, Data curation, Writing – review & editing. **Adebayo A. Adeniyi:** Software, Data curation,

Writing – review & editing. **John Adeolu Falode:** Conceptualization, Software, Data curation. **Tajudeen Olabisi Obafemi:** Investigation, Data curation. **Samuel Olalekan Olusanya:** Software, Data curation. **Linette Twigge:** Software, Data curation, Writing – review & editing. **Jeanette Conradie:** Writing – review & editing. **Timothy O. Mosaku:** Conceptualization.

Declaration of Competing Interest

The authors declare that they have no known competing financial interests or personal relationships that could have appeared to influence the work reported in this paper.

Acknowledgements

Appendix A. Supplementary data

Supplementary data to this article can be found online at https://doi.org/10.1016/j.chmed.2023.01.006.

References

Adebayo, A. H., John-Africa, L. B., Agbafor, A. G., Omotosho, O. E., & Mosaku, T. O. (2014). Anti-nociceptive and anti-inflammatory activities of extract of *Anchomanes difformis* in rats. *Pakistan Journal of Pharmaceutical Science, 27*(2), 265–270.

Adeoye, A. O., Falode, J. A., Jeje, T. O., Agbetuyi-Tayo, P. T., Giwa, S. M., Tijani, Y. O., & Akinola, D. E. (2022). Modulatory potential of *Citrus sinensis* and *Moringa oleifera* extracts and epiphytes on rat liver mitochondrial permeability transition pore. *Current Drug Discovery Technologies, 19*(3). e150322202238.

Adeoye, A. O., Olanlokun, J. O., & Bewaji, C. O. (2018). Activity of apigenin and quercetin on rat hepatic mitochondrial permeability transition pore. *Pharmacology Online, 2*, 11–22.

Akinkurolere, R. O., Adedire, C. O., & Odeyemi, O. O. (2006). Laboratory evaluation of the toxic properties of forest anchomanes, *Anchomanes difformis* against pulse beetle *Callosobruchus maculatus* (Coleoptera: Bruchidae). *Insect Science, 13*, 25–29.

Alessio, H. M. (2000). Lipid peroxidation in healthy and diseased models: Influence of different types of exercise. In *Handbook of Oxidants and Antioxidants in Exercise* (pp. 115–127). Elsevier.

Appaix, F., Minatchy, M. N., Riva-Laveille, C., Olivares, J., Antosson, B., & Saks, V. A. (2000). Rapid spectrophotometric method for the quantitation of cytochrome C release from isolated mitochondria or permeabilized cells revisited. *Biochemical and Biophysical Acta, 1457*, 175–181.

Baines, C. P., Kaiser, R. A., Purcell, N. H., Blair, N. S., Osinska, H., Hambleton, M. A., ... Molkentin, J. D. (2005). Loss of cyclophilin D reveals a critical role for mitochondrial permeability transition in cell death. *Nature, 434*(7033), 658–662.

Bernardi, P., Rasola, A., Forte, M., & Lippe, G. (2015). The mitochondrial permeability transition pore: Channel formation by F-ATP synthase, integration in signal transduction and role in pathophysiology. *Physiological Review, 95*(4), 1111–1155.

Boampong, J. N., Ameyaw, E. O., Aboagye, B., Asare, K., Kyei, S., Donfack, J. H., & Woode, E. (2013). The curative and prophylactic effects of xylopic acid on *Plasmodium berghei* infection in mice. *Journal of Parasitology Research, 356107*.

Bouic, P. J., Etsebeth, S., Liebenberg, R. W., Albrecht, C. F., Pegel, K., & Van Jaarsveld, P. P. P. (1996). Beta-Sitosterol and beta-sitosterol glucoside stimulate human peripheral blood lymphocyte proliferation: Implications for their use as an immunomodulatory vitamin combination. *International Journal of Immunopharmacology, 18*(12), 693–700.

Daniel, O. O., Adeoye, A. O., Ojowu, J., & Olorunsogo, O. O. (2018). Inhibition of liver mitochondrial membrane permeability transition pore opening by quercetin and vitamin E in streptozotocin-induced diabetic rats. *Biochemical and Biophysical Research Communications, 504*, 460–469.

Devendra, C., & Leng, R. A. (2011). Feed resources for animals in Asia: Issues, strategies for use, intensification, and integration for increased productivity. *Asian-Australasian Journal of Animal Sciences, 24*(3), 303–321.

Dubois, M., Vacher, P., Roger, B., Huyghe, D., Vandewalle, B., Kerr-Conte, J., & Lang, J. (2007). Glucotoxicity inhibits late steps of insulin exocytosis. *Endocrinology, 148*, 1605–1614.

Fan, X. Y., Yuan, L., Wu, C., Liu, Y. J., Jiang, F. L., Hu, Y. J., & Liu, Y. (2018). Mitochondrial toxicity: Membrane permeability transition pore opening and respiratory dysfunction. *Toxicology Research, 7*, 191.

Fulda, S. (2010). Modulation of apoptosis by natural products for cancer therapy. *Planta Medica, 76*, 1075–1079.

Halestrap, A. P., McStay, G. P., & Clarke, S. J. (2002). The permeability transition Pore complex: Another view. *Biochimie, 84*, 153–166.

Johnson, D., & Lardy, H. (1967). Isolation of liver or kidney mitochondria. *Methods in Enzymology, 10*, 94–96.

Lapidus, R. G., & Sokolove, P. M. (1993). Spermine inhibition of the permeability transition of isolated rat liver mitochondria: An investigation of mechanism. *Archives of Biochemistry and Biophysics, 306*(1), 246–253.

Li, J. H., Liu, X. R., Zhang, Y., Tian, F. F., Zhao, G. Y., Yu, Q. L., ... Liu, Y. (2012). Toxicity of nano zinc oxide to mitochondria. *Toxicology Research, 1*(2), 137–144.

Lin, S. C., & Way, E. L. (1982). A high-affinity calcium, ATPase enriched nerve ending plasma membrane activated ATPase of brain nerve ending. *Journal of Neurochemistry, 42*, 1697–1706.

Lowry, O. H., Rosebrough, N. J., Farr, A. I., & Randall, R. J. (1951). Protein measurement with the Folin phenol reagent. *Journal of Biological Chemistry, 193*, 262–275.

McKenzie, B. A., Fernandes, J. P., Doan, M. L., Schmitt, L. M., Brandon, W. G., & Power, C. (2020). Activation of the executioner caspase 3 and 9 promotes microglial pyroptosis in models of multiple sclerosis. *Journal of Neuroinflammation, 17*, 1–25.

Morita, N., Sovari, A. A., Xie, Y., Fishbein, M. C., Mandel, W. J., Garfinkel, A., ... Karagueuzian, H. S. (2009). Increased susceptibility of aged hearts to ventricular fibrillation during oxidative stress. *American Journal of Physiology. Heart and Circulatory Physiology, 297*(5), H1594–H1605.

Oyetayo, V. O. (2007). Comparative studies of the phytochemical and antimicrobial properties of the leaf, stem, and tuber of *Anchomanes difformis. Journal of Pharmacology and Toxicology, 2*(4), 407–410.

Rao, V. K., Carlson, E. A., & Yan, S. S. (2014). Mitochondrial permeability transition pore is a potential drug target for neurodegeneration. *Biochimica et Biophysica Acta, 1842*(8), 1267–1272.

Ruberto, G., Baratta, M. T., Deans, S. G., & Dorma, H. J. (2000). Antioxidant and antimicrobial activity of *Foeniculum vulgare* and *Crithmum maritimum* essential oils. *Planta Medica, 66*, 687–693.

Sabeva, N. S., McPhaul, C. M., Li, X., Cory, T. J., Feola, D. J., & Graf, G. A. (2011). Phytosterols differentially influence ABC transporter expression, cholesterol efflux, and inflammatory cytokine secretion in macrophage foam cells. *Journal Nutritional Biochemistry, 22*, 777–783.

Srinivasan, B. (2012). Mitochondrial permeability transition pore: An enigmatic gatekeeper. *New Horizons in Science and Technology, 1*, 47–51.

Strehler, E. E., & Zacharias, D. A. (2001). Role of alternative splicing in generating isoform diversity among plasma membrane calcium pumps. *Physiological Reviews, 81*(1), 21–50.

Yuan, J., Najafov, A., & Py, B. F. (2016). Roles of caspases in necrotic cell death. *Cell, 167*(7), 1693–1694.

Zorov, D. B., Juhaszova, M., & Sollott, S. J. (2014). Mitochondrial reactive oxygen species (ROS) and ROS-induced ROS. *Physiological Reviews, 94*, 909–950.